



# A high-working-temperature CuAlMnZr shape memory alloy

J. Chen<sup>a</sup>, Z. Li<sup>a,b,\*</sup>, Y.Y. Zhao<sup>c</sup>

<sup>a</sup> School of Materials Science and Engineering, Central South University, Lushan South Road, Changsha 410083, China

<sup>b</sup> Key Laboratory of Nonferrous Metal Materials Science and Engineering, Ministry of Education, Changsha 410083, China

<sup>c</sup> Department of Engineering, University of Liverpool, Liverpool L69 3GH, UK

## ARTICLE INFO

### Article history:

Received 13 November 2008

Received in revised form 22 January 2009

Accepted 22 January 2009

Available online 6 February 2009

### Keywords:

Metals and alloys

Shape memory

Phase transitions

Microstructure

## ABSTRACT

The martensitic structure in the air-cooled Cu–11.91Al–2.48Mn–0.1Zr (wt%) alloy and its variation upon heating has been studied by X-ray diffraction and TEM. The forward and reverse thermoelastic transformation behavior has been studied by voltage measurement. The shape memory ratio of the alloy aged at 150 °C (in martensite state) for different times up to 100 h, or heated to different temperatures up to 620 °C followed by air cooling, has been measured. The air-cooled state of the alloy has a monoclinic martensitic structure M18R, which closely matches the N18R structure. This structure remains almost unchanged when the alloy is heated to 400 °C. When the alloy is heated to 620 °C, only a small amount of  $\gamma_2$  phase precipitates and a shape memory ratio of 92% is achieved. When the alloy is aged at 150 °C for 100 h, a shape memory ratio of 97.2% is achieved.

© 2009 Elsevier B.V. All rights reserved.

## 1. Introduction

Cu–Zn–Al and Ni–Ti based alloys are well known to exhibit shape memory effect associated with thermoelastic martensitic transformation [1–3]. While Ni–Ti based shape memory alloys (SMAs) have best properties for most commercial applications, Cu–Zn–Al SMAs are much cheaper than Ni–Ti alloys. However, martensite stabilization is always a problem in Cu–Zn–Al alloys [4–7]. Stabilization may arise from the pinning of the interfaces between martensite and parent phases or between the variants of martensite [8] and from reordering of the martensitic phase during aging [2,9]. One limitation common to both Cu–Zn–Al and Ni–Ti alloys is that their maximum working temperatures are about 100 °C. To overcome this problem, other alloy systems, e.g. Cu–Al–Ni and CuAlNiMnTi SMAs [10–12], have recently been developed for applications at higher temperatures.

In the present study, a new SMA, with a composition of Cu–11.91Al–2.48Mn–0.1Zr (wt %), is developed. This alloy exhibits a good resistance to irreversible martensite stabilization and has a high  $M_s$  temperature of 210 °C. It has potential to be used as a high-temperature smart material for many applications, such as sensors.

## 2. Experimental procedure

The Cu–11.91Al–2.48Mn–0.1Zr (wt%) alloy was prepared by induction melting. The cast ingots were homogenized at 850 °C for 2 h followed by hot-rolling and cold-rolling. Intermediate annealing was carried out at 800 °C for 30 min after every two or three passes. The resulting plate had a final thickness of 1.0 mm. Test specimens were cut from the plate and solution treated at 850 °C for 10 min followed by air-cooling to room temperature. They were then aged at different temperatures for different times and air-cooled to room temperature before being subjected to various tests. The heating-rate to the aging temperature was maintained at 5 °C/min.

The shape memory ratio,  $\eta$ , of the alloy aged at different temperatures and different times was measured using strips with dimensions of 20 mm × 2 mm × 1 mm. Each strip was bent to 90° around a circular cylinder at room temperature as shown in Fig. 1 [13] and then heated above the  $A_f$  temperature. The residual angle was then measured. The shape memory ratio,  $\eta$ , and the maximum deformation strain,  $\varepsilon$ , can be calculated by

$$\eta = \left(1 - \frac{\theta}{90}\right) \times 100\%, \quad \varepsilon = \left(\frac{t}{D+t}\right) \times 100\% \quad (1)$$

where  $\theta$  is residual angle after the sample is heated above the  $A_f$  temperature,  $t$  is the specimen thickness and  $D$  is the diameter of the cylinder, i.e. the diameter of curvature. In this study,  $t = 1$  mm and  $D = 24$  mm; the maximum deformation strain,  $\varepsilon$ , was pre-determined to be 4%.

Microstructure analysis on the test samples was carried out by optical microscopy, transmission electron microscopy (TEM) and X-ray diffraction. The variation of voltage of the sample, when subjected to a constant electric current, as a function of temperature was measured.

## 3. Results

### 3.1. Transformation temperatures

Fig. 2 shows the variation of voltage of a quenched Cu–11.91Al–2.48Mn–0.1Zr sample as a function of temperature in 10 heating-

\* Corresponding author at: School of Materials Science and Engineering, Central South University, Lushan South Road, Changsha 410083, China.  
Tel.: +86 731 8830264; fax: +86 731 8876692.

E-mail address: [lizhou6931@gmail.com](mailto:lizhou6931@gmail.com) (Z. Li).

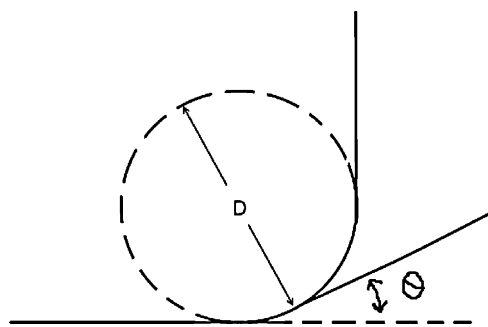


Fig. 1. Schematic plan of the measurement of shape memory ratio.

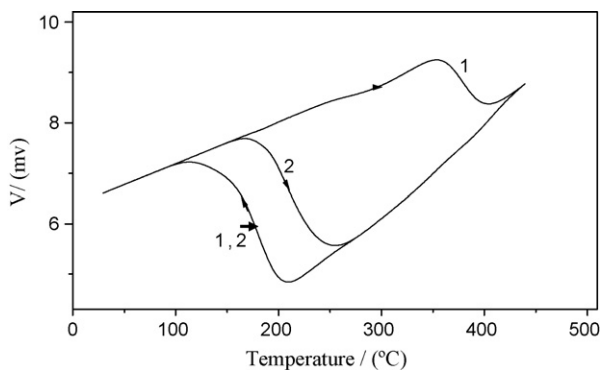


Fig. 2. Voltage-temperature curve of Cu-11.91Al-2.48Mn-0.1Zr alloy. (1) First cycle; (2) second to tenth cycles.

cooling cycles. The heating and cooling rates were maintained at 5 °C/min. The first reverse thermoelastic transformation took place at about 420 °C and the first forward thermoelastic martensitic transformation occurred at about 210 °C upon cooling. In the subsequent cycles, the forward-reverse thermoelastic martensitic transformation became stable and took place between 100 and 275 °C.

### 3.2. Effect of aging on shape memory ratio

Fig. 3 shows the shape memory ratio of the Cu-11.91Al-2.48Mn-0.1Zr samples aged at 150 °C for different times. It is shown that the shape memory ratio decreased gradually with aging time.

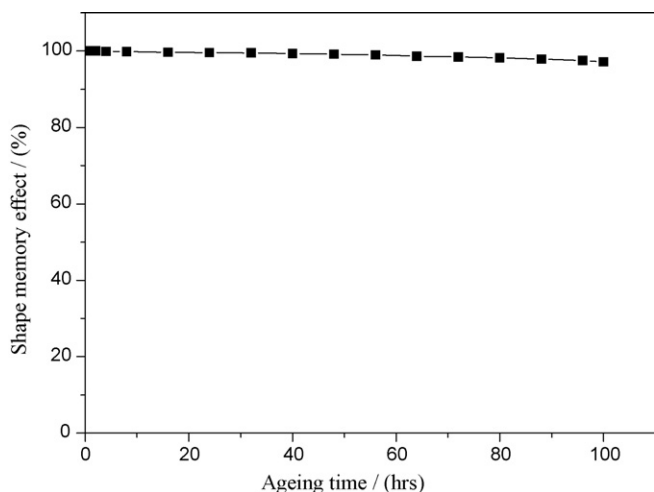


Fig. 3. Shape memory ratio of Cu-11.91Al-2.48Mn-0.1Zr alloy as a function of aging time at 150 °C.

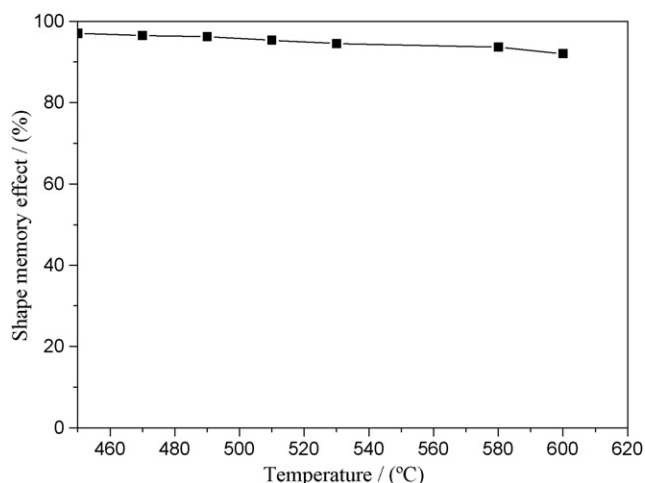


Fig. 4. Shape memory ratio of Cu-11.91Al-2.48Mn-0.1Zr alloy heated to different temperatures and air-cooled to RT.

At an aging time of 100 h, the alloy maintained a shape memory ratio of 97.2%.

Fig. 4 shows the shape memory ratio of the Cu-11.91Al-2.48Mn-0.1Zr samples, which were heated to different temperature at a heating rate of 5 °C/min and immediately air-cooled to room temperature. The shape memory ratio decreased slowly with heating temperature; it remained at 92% as it was heated to 620 °C.

### 3.3. Microstructure observation

The martensitic structure of the alloy after air cooling and heating to 450 °C is shown in Fig. 5(a) and (b), respectively. Formation of  $\gamma_2$ -precipitates only occurred in the martensite phase when it was heated to 450 °C prior to air-cooling to room temperature (Fig. 5(b)). Examination of the air-cooled sample by TEM and ED has shown that it has an M18R type of martensitic crystal structure, the substructure of which is stacking fault (Fig. 6).

### 3.4. X-ray diffraction

The X-ray diffraction profiles of the samples heated to different temperatures at a heating rate of 5 °C/min are shown in Fig. 7. The crystal structure of the air-cooled sample is a modified M18R type martensite, the lattice parameters of which are shown in Table 1. The crystal structure closely matches the N18R structure. It is very interesting to note that two pairs of diffraction peaks, the  $(12l)_M$  and  $(20l)_M$ , as well as  $(040)_M$  and  $(320)_M$ , coincide. Detailed examination of the change of these peaks with temperature shows that: (1) the relative intensities of the  $(111)_M$  and  $(019)_M$  peaks, which are used to judge the nearest-neighbor long-range order ( $L_2$ -type), are nearly independent of the heating temperature (see Table 2); (2) the diffraction profiles of the alloy heated up to 400 °C remain almost the same as that of the air-cooled state; (3) the diffraction peaks of  $\gamma_2$  precipitates only appear when the sample is heated to above 400 °C prior to air-cooling to room temperature and the integrated intensity of these peaks increases slightly with heating temperature.

Table 1  
Lattice parameters of M18R martensite formed in the air-cooled sample.

|             |        |
|-------------|--------|
| $a$ (nm)    | 0.4475 |
| $b$ (nm)    | 0.5229 |
| $c$ (nm)    | 3.814  |
| $\beta$ (°) | 89.62  |

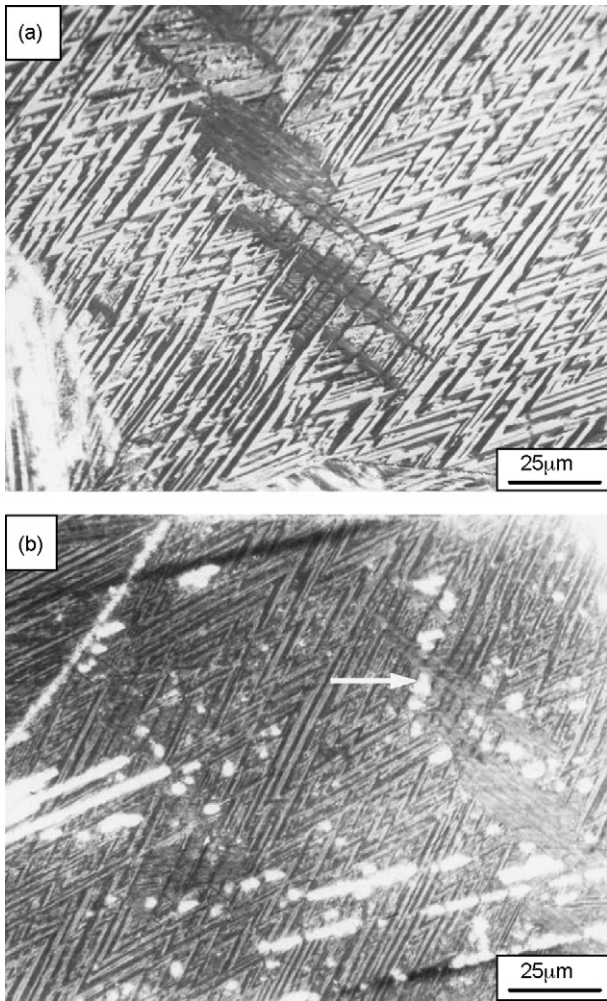


**Fig. 5.** Optical micrographs of Cu–11.91Al–2.48Mn–0.1Zr alloy. (a) As air-cooled and (b) heated to 450 °C prior to air-cooling to RT (polarized light) ( $\gamma_2$  phase is shown by  $\rightarrow$ ).

#### 4. Discussions

The shape memory effect of Cu-based SMAs is associated with thermoelastic transformation from  $B_2$  (or  $DO_3$ ) phase to 9R (or 18R), 3R and 2H martensite, depending on the composition and heat-treatment of the alloy. It was reported that the 9R (or 18R) type martensite has a monoclinic unit cell [14]. When martensite stabilization occurs, the structure of the martensite transforms from monoclinic to orthorhombic [15], and the orthorhombic distortion is attributed to the reordering of the martensitic phase [16]. If the monoclinic angle of the quenched martensite,  $\beta$ , is 90° (orthorhombic) or very close to 90°, the transition from monoclinic to orthorhombic would be restrained and it would be difficult for the martensite stabilization to occur during aging in the martensite state. The martensitic structure in the air-cooled samples of Cu–11.91Al–2.48Mn–0.1Zr alloy closely matches the N18R struc-

**Table 2**

Relatively integrated intensity of  $(111)_M$  and  $(019)_M$  of the samples heated to different temperatures.

|  | Air-cooled state | 160 °C | 280 °C |
|--|------------------|--------|--------|
| $(I_{111}/I_{12\bar{8}}) \times 10^{-2}$ | 6.80             | 6.77   | 6.79   |
| $(I_{019}/I_{12\bar{8}}) \times 10^{-2}$ | 8.60             | 8.61   | 8.62   |

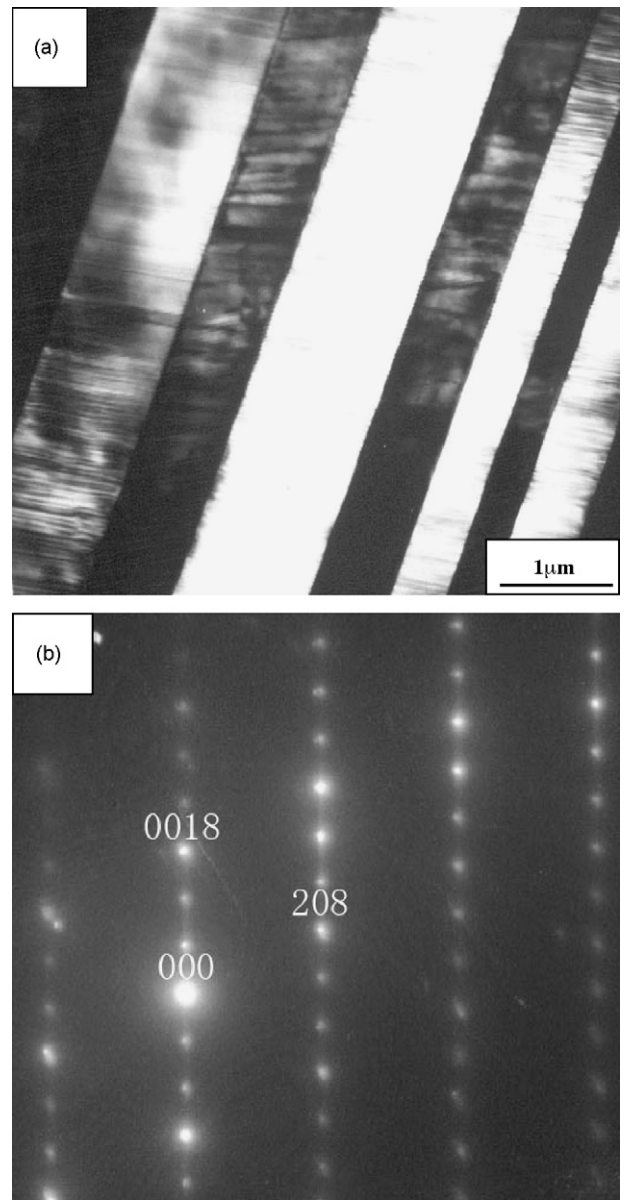


**Fig. 6.** TEM of Cu–11.91Al–2.48Mn–0.1Zr alloy air-cooled. (a) TEM BF and (b) selected ED pattern (zone axis of  $[010]_M$ ).

ture, the variation in orthorhombic distortion in the tested samples of the alloy is less obvious than those found in CuZnAl alloys [16,17].

The alloy exhibits a good resistance to irreversible martensite stabilization. A stable forward-reverse thermoelastic martensitic transformation takes place between 100 and 275 °C after the first thermal cycle. The shape memory ratio is maintained at a high value of 97.2% when the alloy is aged at 150 °C for 100 h. This may also be due to the addition of Mn, which may increase the binding force between the constituent atoms, leading to increased activation energy for diffusion and decreased diffusion rate of the atoms for re-ordering [18].

For the Cu–Zn–Al alloy, the parent phase  $\beta$  either transforms to bainite or directly decomposes into  $\alpha + \gamma_1$  (eutectoid reaction) during aging. This reduces the amount of the parent phase available for martensitic transformation. Consequently, shape memory capacity of the alloy decreases accordingly [18]. For the Cu–Al–Ni alloy [19], the eutectoid decomposition ( $\beta \rightarrow \alpha + \gamma_1$ ) occurs when

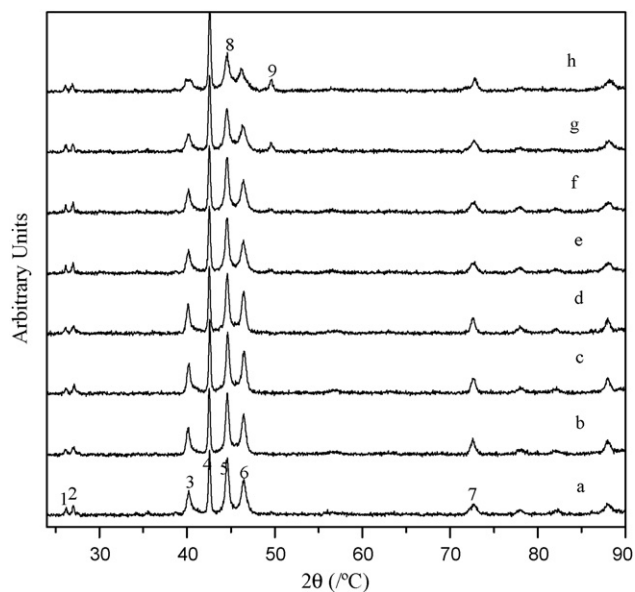


**Fig. 7.** X-ray diffraction profiles of Cu-11.91Al-2.48Mn-0.1Zr alloy, heated to different temperatures followed by air-cooling to room temperature: (a) direct air-cooling, (b) 160 °C, (c) 280 °C, (d) 400 °C, (e) 450 °C, (f) 500 °C, (g) 550 °C, and (h) 600 °C. (1) 111, (2) 019, (3)  $12\bar{2}(202)$ , (4) 0018, (5)  $12\bar{8}(208)$ , (6) 1210 ( $20\bar{1}0$ ), (7) 040 ( $320$ ), (8) 208 ( $(330)_{\gamma_2}$ ,  $(411)_{\gamma_2}$ ), and (9)  $322_{\gamma_2}$ .

heated to 550 °C. Only 10% of the  $\beta$  phase remained untransformed, resulting in a significantly decreased mass fraction of thermoelastic martensite. For the Cu-Al-Ni-Mn-Ti alloy [20], bainite is precipitated at about 300 °C, resulting in a drastic depression in martensitic transformation temperatures and loss of the shape memory capacity.

The parent phase of the Cu-11.91Al-2.48Mn-0.1Zr alloy is stable and does not decompose easily during aging. A high shape memory ratio of 92% was achieved when the alloy was heated to 620 °C. This can be explained by the fact that addition of Mn to Cu-Al alloys helps to stabilize the  $\beta$  phase and widen the  $\beta$  phase region [21]. According to the Cu-Al binary phase diagram [22], the  $\beta$  phase is stable in the composition range from 20 to 30 at% Al at temperatures higher than about 560 °C. A composition with 11.91 wt% of Al, in the tested alloy, is close to the eutectic composition of the binary Cu-Al alloy. Addition of 2.48 wt% Mn to the Cu-Al alloy stabilizes the  $\beta$  phase and widens the  $\beta$  phase region. As a result, only a small quantity of  $\gamma_2$  precipitates is present when the alloy is heated to 620 °C. The eutectoid reaction ( $\beta \rightarrow \alpha + \gamma_1$ ) does not take place.

## 5. Conclusions

Monoclinic martensitic structure M18R is observed in the air-cooled Cu-11.91Al-2.48Mn-0.1Zr samples, which closely matches the N18R structure. When the alloy is heated to a temperature up to 400 °C, the martensitic structure remains almost the same as that of the quenched state. When the alloy is heated to 620 °C, only a small amount of  $\gamma_2$  phase precipitates and the eutectoid reaction ( $\beta \rightarrow \alpha + \gamma_1$ ) does not take place; a shape memory ratio of 92% is achieved. When the alloy is aged at 150 °C for 100 h, a shape memory ratio of 97.2% is achieved.

In the first thermal cycle, the reverse thermoelastic transformation takes place at about 420 °C upon heating, and the forward thermoelastic martensitic transformation occurs at about 210 °C upon cooling. A stable forward-reverse thermoelastic martensitic transformation takes place between 100 and 275 °C during the subsequent thermal cycles.

## Acknowledgments

This study was supported by the Natural Science Foundation of Hunan Province (05JJ30095) and Ph.D. Programs Foundation of Ministry of Education of China (20040533069).

## References

- [1] K. Otsuka, X.B. Ren, *Intermetallics* 7 (1999) 511–528.
- [2] J.W. Xu, *J. Alloys Compd.* 448 (2008) 331–335.
- [3] V.G. Pushin, A.I. Lotkov, Yu.R. Kolobov, R.Z. Valiev, E.F. Dudarev, N.N. Kuranova, A.P. Dyupin, D.V. Gunderov, G.P. Bakach, *Phys. Met. Metall.* 106 (2008) 520–530.
- [4] A. Cuniberti, R. Romero, M. Stipcich, *J. Alloys Compd.* 472 (1–2) (2009) 162–165.
- [5] M. Ahlers, *Mater. Sci. Eng. A* 349 (2003) 120–131.
- [6] K. Otsuka, X. Ren, *Scripta Mater.* 50 (2004) 207–212.
- [7] M. Ahlers, *Mater. Sci. Eng. A* 481–482 (2008) 500–503.
- [8] S. Kustov, J. Pons, E. Cesari, J. Van Humbeeck, *Acta Mater.* 52 (2004) 3083–3096.
- [9] S. Kustov, J. Pons, E. Cesari, J. Van Humbeeck, *Acta Mater.* 52 (2004) 4547–4559.
- [10] N. Suresh, U. Ramamurty, *J. Alloys Compd.* 449 (2008) 113–118.
- [11] L. Delaey, *Phase Transformation in Materials*, Weinheim, Germany, 1991.
- [12] R. Fernández, A.V. Benedetti, J.M. Guilemany, X.M. Zhang, *Mater. Sci. Eng. A* 438–440 (2006) 723–725.
- [13] S.M. Tang, C.Y. Chung, W.G. Liu, *J. Mater. Process. Technol.* 63 (1997) 307–312.
- [14] F. Saule, M. Ahlers, F. Kropef, E.B. Rivero, *Acta Metall.* 40 (12) (1992) 3229–3238.
- [15] A. Abu Arab, M. Ahlers, *Acta Metall.* 36 (1988) 2627–2638.
- [16] F. Saule, M. Ahlers, *Acta Metall.* 43 (1995) 2373–2384.
- [17] T. Suzuki, R. Kojima, Y. Fujii, A. Nagasawa, *Acta Metall.* 37 (1989) 163–168.
- [18] C.Y. Chung, C.W.H. Lam, S.S. Tan, *Mater. Lett.* 33 (1998) 291–296.
- [19] V. Recarte, J.I. Pérez-Landazábal, A. Ibarra, M.L. Nó, J. San Juan, *Mater. Sci. Eng. A* 378 (2004) 238–242.
- [20] Z.G. Wei, H.Y. Peng, W.H. Zou, *Metall. Mater. Trans. A-Phys. Metall. Mater. Sci.* 28 (1997) 955–967.
- [21] R. Kainuma, N. Satoh, X.J. Liu, I. Ohnuma, K. Ishida, *J. Alloys Compd.* 266 (1998) 191–200.
- [22] V. Recarte, J.I. Pérez-Landazábal, A. Ibarra, *Mater. Sci. Eng. A* 378 (2004) 238–242.